

Improving coherent contrast of petawatt laser pulses

Chris Hooker,^{1,2} Yunxin Tang,¹ Oleg Chekhlov,¹ John Collier,¹ Edwin Divall,¹ Klaus Ertel,¹ Steve Hawkes,¹ Bryn Parry,¹ and P. P. Rajeev^{1,*}

¹Central Laser Facility, Rutherford Appleton Laboratory, Harwell Science and Innovation Campus, Didcot, Oxfordshire OX11 0QX, U.K.

²Chris.Hooker@stfc.ac.uk

*Rajeev.Pattathil@stfc.ac.uk

Abstract: We report on an experimental study of the “coherent” contrast feature that frequently appears in petawatt(PW)-class laser pulses as an exponentially-rising pedestal within a few tens of picoseconds of the compressed pulse. We show that scattering from the diffraction gratings in the stretcher is the principal source of this feature. Replacing the gratings by new, higher-quality components resulted in an order-of-magnitude reduction in the intensity of the pedestal.

© 2011 Optical Society of America

OCIS codes: (050.0050) Diffraction and Gratings; (320.5520) Pulse compression ; (290.5880) Scattering, rough surfaces.

References and links

1. D. Neely, P. Foster, A. Robinson, F. Lindau, O. Lundh, A. Persson, C.-G. Wahlström, and P. McKenna, “Enhanced proton beams from ultrathin targets driven by high contrast laser pulses,” *Appl. Phys. Lett.* **89**, 021502 (2006).
2. C. Hernandez-Gomez, S. P. Blake, O. Chekhlov, R. J. Clarke, A. M. Dunne, M. Galimberti, S. Hancock, R. Heathcote, P. Holligan, A. Lyachev, P. Matousek, I. O. Musgrave, D. Neely, P. A. Norreys, I. Ross, Y. Tang, T. B. Winstone, B. E. Wyborn, and J. Collier, “The Vulcan 10 PW Project,” *J. Phys.* **244** 032006 (2010).
3. <http://www.extreme-light-infrastructure.eu>.
4. D. Strickland and G. Mourou, “Compression of amplified chirped optical pulses,” *Opt. Commun.* **56**, 219–221 (1985).
5. M. P. Kalashnikov, E. Risse, H. Schönengel, and W. Sandner, “Double chirped-pulse-amplification laser: a way to clean pulses temporally,” *Opt. Lett.* **30**, 923–925 (2005).
6. A. Jullien, O. Albert, F. Burgy, G. Hamoniaux, J.-P. Rousseau, J.-P. Chambaret, F. Augé-Rochereau, G. Cheriaux, J. Etchepare, N. Minkovski, and S. M. Satiel, “ 10^{-10} temporal contrast for femtosecond ultraintense lasers by cross-polarized wave generation,” *Opt. Lett.* **30**, 920–922 (2005).
7. A. Lévy, T. Ceccotti, P. D’Oliveira, F. Réau, M. Perdrix, F. Quéré, P. Monot, M. Bougeard, H. Lagadec, P. Martin, J.-P. Geindre, and P. Audebert “Double plasma mirror for ultrahigh temporal contrast ultraintense laser pulses,” *Opt. Lett.* **32**, 310–312 (2007).
8. H. P. Weber and R. Dändliker, “Method for measurement the shape asymmetry of picosecond light pulses,” *Phys. Lett.* **28A**, 77–78, (1968).
9. M. Kalashnikov, K. Osvay, and W. Sandner, “High-power Ti:sapphire lasers: temporal contrast and spectral narrowing,” *Laser Part. Beams* **25**, 219–223(2007).
10. K. H. Hong, B. Hou, J. A. Nees, E. Power, and G. Mourou, “Generation and measurement of $> 10^8$ intensity contrast ratio in a relativistic kHz chirped-pulse amplified laser,” *Appl. Phys. B* **81**, 447–457 (2005).
11. K. Osvay, M. Csatari, I. N. Ross, A. Persson, and C.-G. Wahlström, “On the temporal contrast of high intensity femtoseconds laser pulses,” *Laser Part. Beams* **23**, 327–332 (2005).
12. D. N. Schimpf, E. Seise, J. Limpert, and A. Tünnemann, “Decrease of pulse-contrast in nonlinear chirped-pulse amplification systems due to high-frequency spectral phase ripples,” *Opt. Express* **16**, 8876–8886 (2008).
13. V. Bagnoud and F. Salin, “Influence of optical quality on chirped-pulse amplification: characterization of a 150-nm-bandwidth stretcher,” *J. Opt. Soc. Am. B* **16**, 188–193(1999).
14. C. Dorrer and J. Bromage, “Impact of high-frequency spectral phase modulation on the temporal profile of short optical pulses,” *Opt. Express* **16**, 3058–3068 (2008).

15. I. N. Ross, A. J. Langley, and P. Taday, "A Simple Achromatic Pulse Stretcher," CLF Annual Report 201–203 (1999–2000), RAL-TR-2000-034.
 16. J. C. Stover, *Optical Scattering Measurement and Analysis*, 2nd. ed. (SPIE Publications. 1995), ISBN13: 9780819477767.
 17. M. Kalashnikov, A. Andreev, and H. Schönagel, "Limits of the temporal contrast for CPA lasers with beams of high aperture," *Proc. SPIE* **7501**, 750104 (2009).
-

1. Introduction

In ultra-intense laser systems used for plasma physics research, contrast is one of the most important properties of the laser pulse. If the pulse has low contrast, a plasma can be formed on the target before the ultrashort compressed pulse arrives, which significantly changes the nature of the interaction [1]. In these circumstances certain types of target, such as ultrathin foils used for ion acceleration, can be completely destroyed prior to the arrival of the main pulse. As future lasers increase in power to tens of PW [2] or exawatts [3], corresponding improvements in pulse contrast will be essential.

The majority of ultra-intense lasers are based on the technique of chirped-pulse amplification (CPA) [4]. In CPA lasers, poor contrast can take the form of amplified spontaneous emission extending over nanoseconds, and discrete prepulses that are usually within a few hundred picoseconds of the main pulse. A third contribution is uncompressible energy within the stretched pulse, which manifests itself as an exponentially-rising pedestal, typically within 20 picoseconds of the main pulse. This latter feature is termed the "coherent" contrast pedestal, and is of concern because its effect is to extend the leading edge of the pulse by several picoseconds at an intensity which is likely to be well above the plasma generation threshold, leading to the damaging effects noted above. Various pulse cleaning techniques such as double CPA [5], XPW [6] and the use of plasma mirrors [7] can significantly improve the contrast on timescales from nanoseconds down to tens of picoseconds, but they become ineffective closer to the main pulse. For this reason it is important to understand the origins of the coherent pedestal (CP) and to find ways of reducing it.

In this paper we report a detailed study of the cause of the CP in Astra Gemini, a petawatt-class Titanium-sapphire laser at the Central Laser Facility in the U.K. The design of the Astra pulse stretcher allowed us to separate the effects of different optical components, and show that the majority of the CP originates from the stretcher gratings.

2. Description of Astra and Gemini

Astra is a 20 Terawatt CPA laser system based on Titanium-sapphire. Gemini is an additional power amplification stage where the output of Astra is split and amplified to yield two synchronised 0.5PW pulses. A schematic block diagram of the Astra Gemini system is shown in Figure 1. The front end consists of a commercially-made 20 fs oscillator, followed by a kHz multi-pass preamplifier in which individual pulses are amplified to the millijoule level. A train of pulses at 10 Hz is selected from the kHz pulse train using a fast Pockels cell, and sent to the Astra pulse stretcher. The pulse stretcher is set up as a cavity in a manner similar to a regenerative amplifier, and each pulse is switched into the stretcher by a Pockels cell positioned between two crossed polarizers. The pulse can be switched out again after either one or two passes through the stretcher, giving either a single stretch of 530 ps for use in the Astra experimental area or a double stretch of 1060 ps if the pulse will be sent to Gemini. The longer stretch is necessary for Gemini to reduce the nonlinear phase integral (B integral) at the output to an acceptably low level. These pulses have a FWHM spectral width of 42 nm. The geometry of the pulse stretcher limits the full spectral width of the stretched pulses to 132nm.

The stretcher is set up as a cavity in a manner similar to a regenerative amplifier, and each

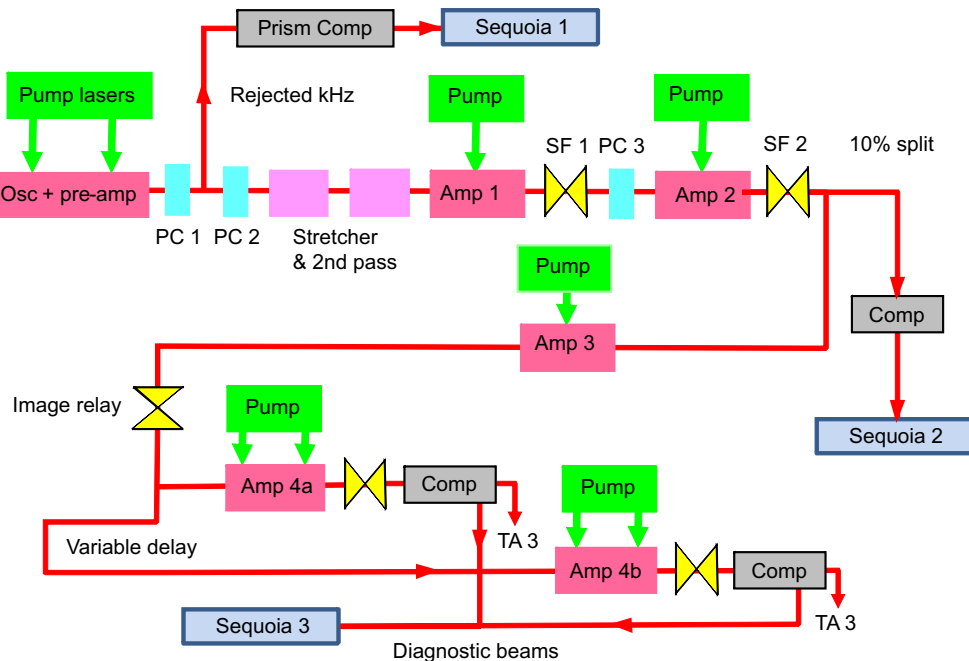


Fig. 1. Schematic block diagram of the Astra-Gemini laser system. The three points where the contrast measurements can be carried out are indicated.

pulse is switched into the stretcher by a Pockels cell positioned between two crossed polarizers. The pulse can be switched out again after either one or two passes through the stretcher, giving either a single stretch of 530 ps for use in the Astra experimental area or a double stretch of 1060 ps if the pulse will be sent to Gemini. The longer stretch is necessary for Gemini to reduce the nonlinear phase integral (B integral) at the output to an acceptably low level.

Following the stretcher there is a chain of three multi-pass Ti:sapphire amplifiers, pumped by Q-switched frequency-doubled Nd:YAG lasers. The output of the third amplifier is sent to the Gemini laser area, where it is split into two beams to seed the two large-aperture amplifiers. The lasers that pump these amplifiers can fire as often as one pulse every 20 seconds, but are run only to provide full energy shots. For diagnostic purposes, the compressed unamplified 10 Hz pulses are available at the output of the pulse compressors, where a sub-diameter beam emerges from the compressor vacuum chamber through a 2 mm thick window to minimise the amount of stretch. This beam has a few mJ of energy per pulse, and was used for the majority of the contrast measurements reported in this study.

3. Contrast measurement

The most widely-used technique for contrast measurement is third-order correlation [8]. In this method, the laser beam is split into two parts, one of which is converted to the second harmonic in a nonlinear crystal. The second-order harmonic process yields a pulse that is relatively clean and free from additional pulses, which is then mixed with the remainder of the original pulse in a second crystal tuned for sum- or difference-frequency generation. The contrast can be mapped as a function of delay by one of two methods. One or both of the pulse fronts can be tilted in order to give a spatially-varying delay, thereby mapping a time window onto the spatial coordinate. Imaging the third harmonic signal then yields a single-shot measurement of the

contrast as a function of delay, which is most useful for laser systems with low repetition rates. Alternatively, the pulses can be scanned through one another using an adjustable relative delay, and the third harmonic signal recorded for each delay to give a plot of contrast versus time. This technique is suitable for repetitively-pulsed lasers, and is used in a well-known commercially available device for measuring contrast: (Amplitude Technologies' Sequoia).

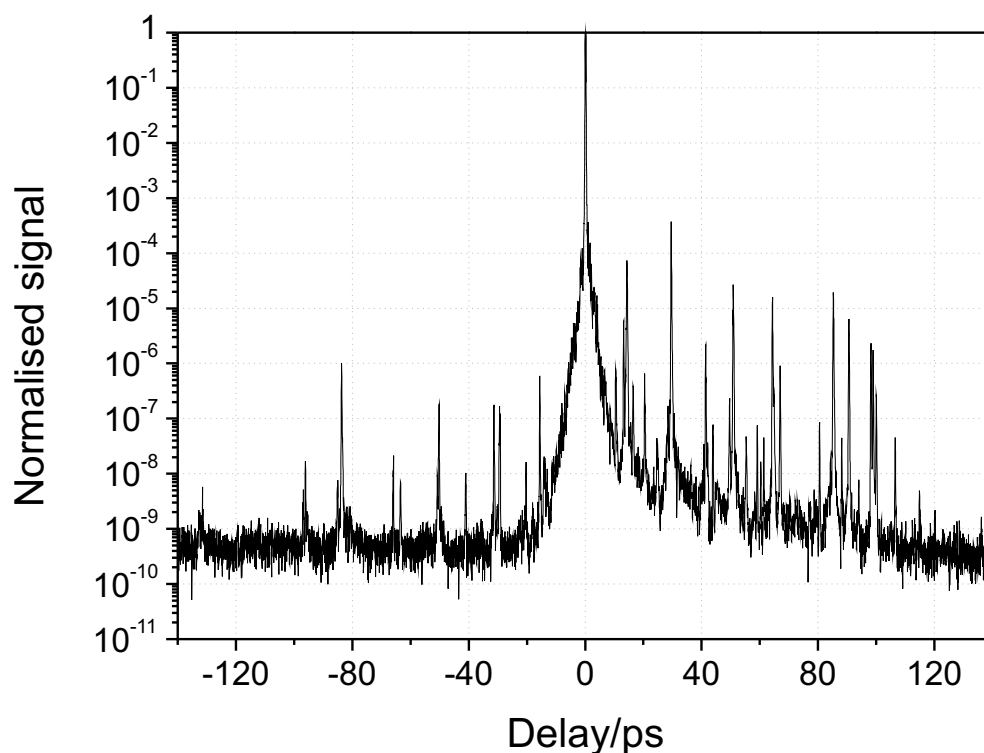


Fig. 2. Typical contrast scan of the Astra 10 Hz beam.

A typical contrast scan obtained with a Sequoia is shown in Figure 2. This scan was made using the Astra Ti:sapphire laser, operating at 10 Hz. It shows three distinct features of contrast: the ASE baseline at around 10^{-9} , various discrete pre- and post-pulses and a triangular pedestal occupying the 10 picoseconds either side of the main pulse. The latter feature is the CP which is the subject of this paper. Similar scans have been published for other Ti:sapphire CPA laser systems [9, 10, 11], and they show very similar features. We have made significant progress in determining the origin of this feature and in reducing it.

4. Experimental study of the coherent pedestal

Determining the origin of the CP is difficult in a CPA laser because contrast measurements can be made only on a compressed pulse. Pulses in the rejected kHz train from the front end of Astra have been stretched to a few picoseconds by material dispersion, and can be recompressed using a prism compressor. A contrast scan of these pulses shows no evidence of the CP, so the source must lie further down the laser chain. This agrees with evidence from other systems where the pulse is not stretched [6]. Once the pulse has passed through the stretcher it must be recompressed before the contrast can be measured, and this requires a full-sized grating compressor, which in our system restricts the locations where the measurement can be made

to the Astra experimental area and the output of the Gemini compressor, as indicated in Fig. 1. Contrast measurements in either place show a fully-developed pedestal on the pulse (Fig. 3), which appears identical regardless of whether the pulse has been stretched to only 530 ps, or to 1.06 ns by passing twice through the stretcher optics. The traces shown were obtained several months apart and with two different pulse compressors. It is extremely unlikely that two different compressors with different geometries and compensating two widely different stretches would introduce pedestals that are so similar. This shows that the compressor gratings make a negligible contribution to the CP.

As with the majority of data presented in this study, these scans were obtained using the 10 Hz beam from Astra alone, operating in the 10 TW regime. However, we have verified that the contrast remains essentially the same even with full power amplification in Gemini. The data points in Figure 3 show the contrast measurements done at full-energy (12 Joules) laser shots, using the same Sequoia device as for all the other contrast scans. The agreement between the 10 TW and full-energy data shows that the additional amplification in Gemini does not degrade the contrast significantly, and thus our conclusions based on 10TW pulses apply equally to the petawatt regime.

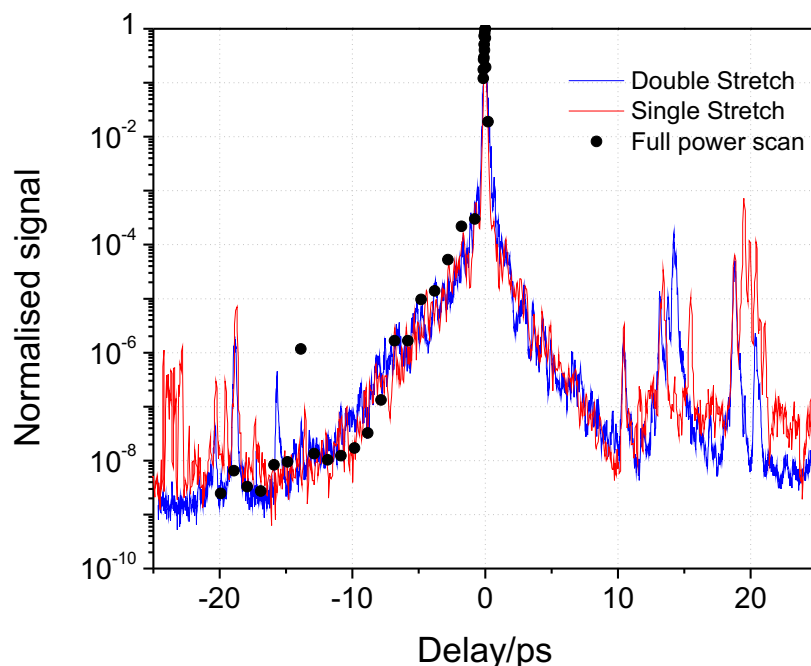


Fig. 3. Measurements of the coherent pedestal of singly stretched (red trace) and doubly stretched (blue trace) pulses from Astra. The black dots show result of a full power contrast measurement in Gemini.

Since the first observation of the CP in Astra in 2006, the laser has undergone many changes, including a complete change of oscillator and preamplifier, a redesign and rebuild of the first amplifier and the introduction of single- and double-pass operation of the pulse stretcher. The CP has remained present throughout and has not been affected by any of these changes. In itself this is a clue that the feature's origin is one of the parts of the laser that has not been

changed, which restricts it to the pulse stretcher, the second amplifier and some of the intervening optics. This is consistent with theoretical work [12, 13, 14], which showed that noise in the spectrum caused by surface roughness of optical components where the beam is spatially dispersed can lead to the appearance of features with this form. This strongly suggests that the CP may originate in the stretcher.

A schematic layout of our pulse stretcher is shown in Fig. 4: part (a) shows a plan view, and part (b) a side view. The spherical mirror is 35 cm in diameter, and the second grating 33 cm wide. The path followed by the beam is normally G1-SM-G2-BM-G2-SM-G1, which is indicated in Figure 4(b) by the red line. This stretcher is not the usual Öffner design, but was developed independently at the CLF [15]. However, laser systems elsewhere that use Öffner-type stretchers exhibit similar contrast features in their compressed pulses [5], so it seems that the design of stretcher does not greatly affect the appearance of the CP.

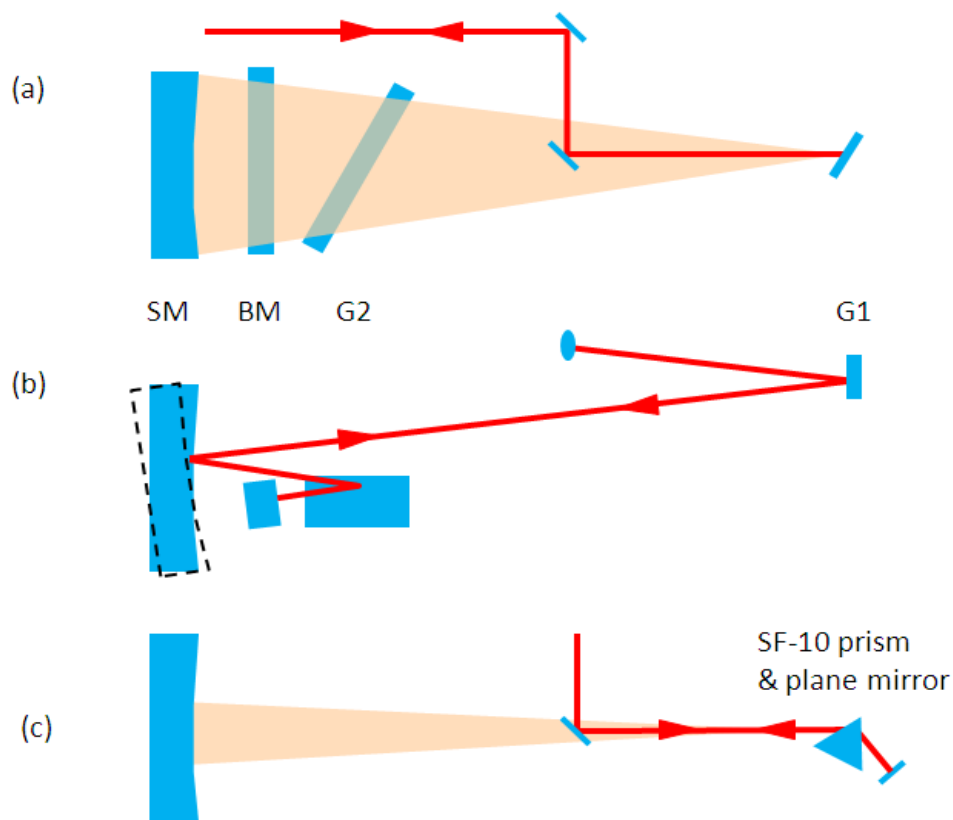


Fig. 4. Diagrams of the Astra pulse stretcher: (a) plan view; (b) side view. Labelled components are: first grating (G1); spherical mirror (SM); second grating (G2); back mirror (BM). The dashed outline in (b) indicates the tilted position of the spherical mirror that was used to bypass the second grating and the back mirror. Part (c) shows a plan view of the prism and mirror arrangement that was used as a substitute for the first grating in the tilted mirror configuration.

We carried out an extensive set of tests in which components of the stretcher were changed or bypassed entirely, with the aim of determining which of them gave rise to the CP. The first optic replaced was the plane back mirror, BM, which had acquired a significant amount of dust and other contamination. Cleaning the surface using strippable polymer made an obvious difference

to the visual appearance but did not affect the CP in any way. It was replaced by a new mirror with a broadband dielectric coating, but this made no difference to the CP either. Replacement of the gold-coated input mirror with a new dielectric-coated optic also made no difference.

The design of the Astra pulse stretcher allows some of the components to be bypassed with suitable realignment. The point of incidence of the beam on the first grating is very close to the centre of curvature of the spherical mirror, so by tilting the mirror up as shown by the dashed outline in Figure 4(b) the dispersed light from the grating can be retro-reflected back to the same point on the grating. The effect is to reverse the dispersion and recollimate the spectral components into a small beam without introducing any time delay between them. This allows the pulse to be compressed in the prism compressor. With this arrangement the beam is not reflected from the second grating or the back mirror, so neither of them has any effect on the contrast.

The result of this test was striking [Figure 5]. The size of the CP was reduced significantly, so that the point where it intersected the rising edge of the main pulse was a factor of 100 lower than on the reference scan. This result demonstrates that a significant part of the CP is due to the second grating, as we previously found that cleaning and then replacing the back mirror had no measurable effect. The residual CP, shown by the red trace in Figure 5, could be due to either the first grating or the spherical mirror. In order to investigate further, we set up a double-passed prism of SF-10 glass and a plane mirror to replace the first grating, in the arrangement shown in plan view in Figure 4(c). The aim was to eliminate the first grating while still dispersing the light on the surface of the spherical mirror

A contrast scan with this arrangement is presented as the blue trace in Figure 5. The main pulse is longer than before, because the dispersion from the approximately 4 cm of path in the SF-10 prism could not be fully compensated in the prism compressor. This resulted in a rise in the level of the baseline, as the signal is normalised to the height of the peak. However, substituting the prism for the grating has reduced the CP by at least another order of magnitude, otherwise it would be visible at the leading edge of the main pulse between -4 and -2 picoseconds. This shows that the residual CP seen when the second grating was bypassed did indeed originate from the first grating, and not from the spherical mirror, which was still present.

The above results conclusively show that only the gratings in the stretcher contribute to CP. Previous theoretical work has shown [12, 13, 14] that spectral phase noise in dispersed beams in stretchers can form exponential pedestals like these. Such spectral phase noise can arise from surface roughness of components where the beam is spatially dispersed. This could account for the observed effect of the second grating. However, there is clearly a contribution to the CP from the first grating where the beam is not dispersed. We also observe that cleaning the back mirror, where the beam is dispersed, did reduce the scatter but did not affect the CP. This leads to the conclusion that scattering from gratings, irrespective of the beam dispersion on them, leads to the formation of CP. It may be that the processes involved in manufacturing diffraction gratings generate roughness on a spatial scale which causes the CP, a roughness that is not present on the optically polished and coated surfaces of mirrors and prisms.

The origin of CP is, however, closely linked with dispersion. When gratings disperse light, wavelength components scattered from the gratings could find a slightly shorter path through the stretcher optics. Such scattered light could leave either grating at a range of angles which would be different from the diffraction angle (for any given wavelength), and could, in principle, travel along a shorter path through the stretcher back to the first grating. The acceptance angle into the subsequent optics would restrict the range of delays that could propagate further down the laser chain. This could account for our observation that the size and shape of the CP remain unchanged regardless of whether the pulse is singly or doubly stretched. We note that the CP has an exponential form, appearing linear in the logarithmic plots, and that typical

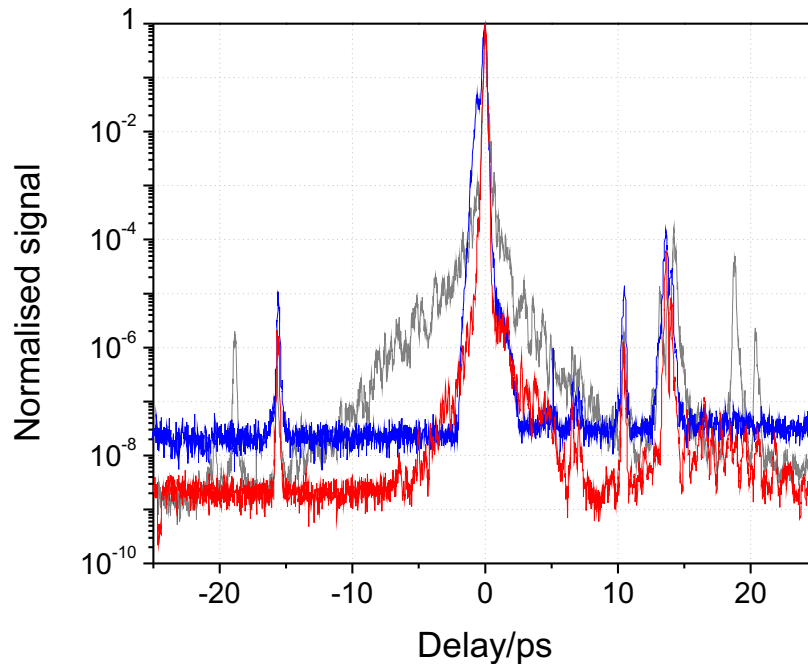


Fig. 5. Comparison of contrast scans with different configurations of the stretcher. Red trace: second grating and back mirror bypassed. Blue trace: prism and mirror in place of first grating. The grey background trace was recorded with the normal configuration of the stretcher.

scatter distribution functions also show an exponential variation with angle [16].

5. Scatter measurements on the gratings

The results described above highlighted the need to replace the gratings in the stretcher. While doing this, we made some simple scatter measurements: on the new gratings before installation and on the old gratings after they were removed from the stretcher. To make the measurements, the grating was mounted with its dispersion direction horizontal, and a fibre-coupled 800 nm CW diode laser with a collimated 3 mm diameter beam was incident on it at the Littrow angle of approximately 36 degrees. The beam was horizontally polarized to match the condition in the stretcher. An infra-red sensitive CCD camera was used to image the laser spot on the grating in scattered light. The angle of view of the camera relative to the beam was kept constant at 1.9 degrees for each grating tested. In the stretcher itself the relevant scattering angles would be of the order of milliradians, but scatter measurements at such a small angle are very difficult to perform. In this case our aim was simply to compare the amount of scattering from new and old gratings under the same conditions, rather than measure their scatter distribution functions accurately.

To measure the scatter, the peak brightness signal in the image of the spot was recorded for a range of different lens apertures and exposures. The exposure time and lens aperture were adjusted while viewing a line-out through a live image of the scatter spot to ensure the image

was not saturated. By comparing the signals obtained at the same exposure and aperture from the new and old gratings, the relative scatter level could be determined. The camera gain and other parameters were kept constant throughout. The data for the old and new second gratings are shown in Table 1.

Table 1. **Relative scattering measurements**

		New Grating 2	Old Grating 2	
Exposure/ms	Aperture	Peak brightness	Peak brightness	Brightness Ratio
10	F/4	151	900	6.0
10	F/5.6	75	520	6.9
10	F/8	46	310	6.7
5	F/2.8	150	930	6.2
5	F/4	74	480	6.5
5	F/5.6	38	260	6.8

There is clearly a significant difference between the two gratings, with the old grating scattering on average 6.5 times more strongly than the new. A similar measurement on the two first gratings showed a smaller factor of 2.5, with the old grating again having the larger scatter.

6. Replacement of stretcher gratings

The original gratings are gold-coated holographic photoresist gratings with a sinusoidal groove shape. The two new gratings were obtained from Plymouth Grating Laboratories, and are etched binary gratings, which have an approximately rectangular groove shape. The grating structure is first formed in photoresist, then etched into the silica substrate before being gold coated. This process improves the damage resistance, and the rectangular groove form also gives significantly higher diffraction efficiency in the 750-850 nm spectral region: the average efficiency measured at 805 nm is 94% in first order for the new second grating, and 91.5 % for the first. Interferometer measurements show that the new second grating has an excellent figure, with a peak-to-valley error of 0.09 wave and an RMS error of 0.013 wave. The old grating has a peak-to-valley error of 0.25 wave and an RMS error of 0.035, which is significantly worse, although the P-V error appears mainly as an overall smooth curvature of the surface.

After installing the new gratings and optimising the pulse duration, a contrast scan was made, which is shown in Figure 6. With the new gratings the level of the CP was reduced by more than an order of magnitude. More accurately, taking the ratio of the signal levels at each delay and averaging them gives a factor of 21 for the reduction in amplitude of the CP. We note this factor is similar to the product of the relative scattering factors of the gratings measured above, which supports our conclusion that scattering from gratings is the principal factor in the origin of the CP.

Although any increase in scattering from the gratings will contribute to the CP, small differences are difficult to detect on a logarithmic scale in a Sequoia trace, especially in the presence of noise. Double-passing the stretcher can at most double the amount of scattered light relative to the main pulse, and the resulting factor of two increase in the CP would be practically undetectable. This is why the single and double passed stretcher configurations have similar CPs, as shown in Figure 3.

Having studied the CP that originates from light scattered by the stretcher gratings, we need

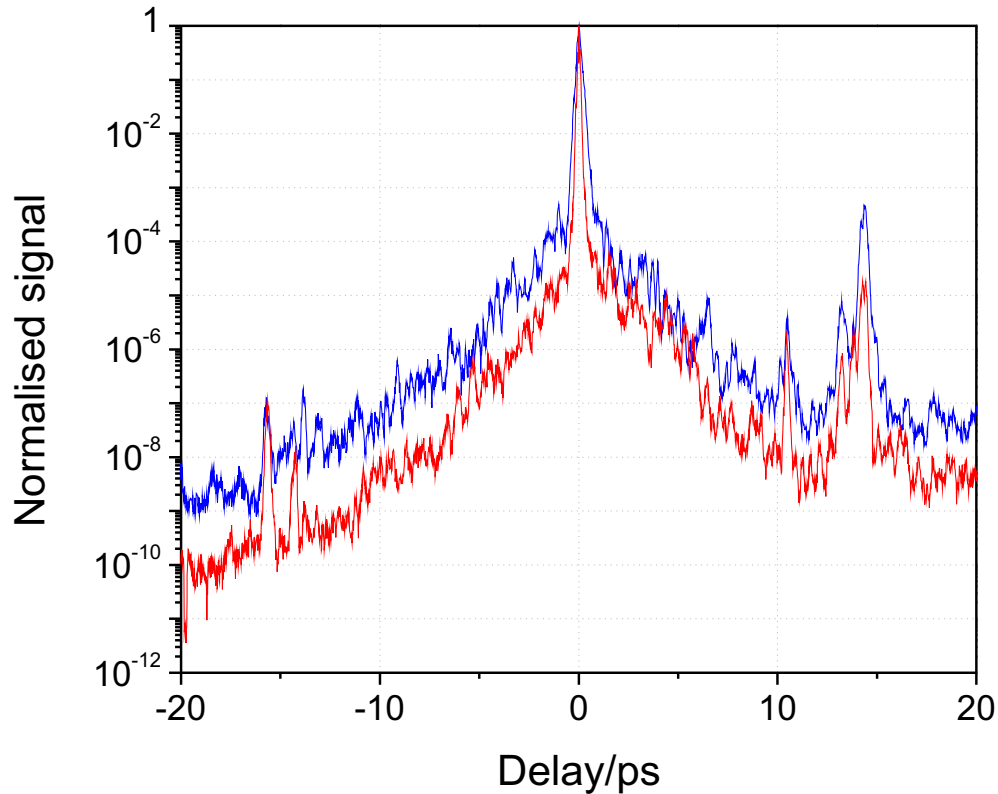


Fig. 6. The coherent pedestal recorded with the original stretcher gratings (blue trace) and the new gratings (red trace).

to consider what effect the compressor gratings have. The traces shown in Figure 3 were obtained with two very different compressors, one with new gratings and the other with old gratings similar to those removed from the stretcher. We might expect to see a significant difference in the corresponding pedestals, as occurred when the stretcher gratings were changed. The close similarity of the traces demonstrates that the compressor gratings have little effect on the level of the pedestal. This agrees with theoretical results [17], which include the statistical effects of averaging over the surface irregularities of the compressor gratings when the beam size is large (150 mm in the case of Gemini). The monochromatic spot size in the stretcher, in comparison, is of the order of 1 mm. The minimal effect of the compressor gratings is encouraging for the development of large high-intensity laser systems, if the generation of the CP in the stretcher can be prevented.

7. Conclusions

We have investigated the origin of the coherent contrast pedestal of a petawatt-class Titanium-sapphire laser system. By making contrast measurements with several optical configurations of the pulse stretcher, in which different components were eliminated or replaced, we were able to distinguish the contribution to the CP from different optics. Our results show that scatter from the diffraction gratings in the pulse stretcher is the main source of the CP. Scatter from mirrors, and dispersion by a prism with polished surfaces, did not make a measurable contribution to the CP. The essential factor in generating a CP therefore appears to be scatter from a dispersing

component.

Installing new higher quality gratings in the Astra pulse stretcher has resulted in an order-of-magnitude reduction in the intensity of the CP, a significant improvement in the overall contrast of the compressed pulse from the laser. The new gratings are etched into the fused silica substrates, rather than being formed in a photoresist layer. The etching process may reduce the roughness of the grating surface, giving lower scatter and leading to the observed improvement in contrast. In the ten or more years since the original gratings were made the technology of grating production has advanced in response to the requirements for high-energy CPA lasers, and gratings made today undoubtedly have better quality. Our results suggest, however, that further improvements may be essential, as the coherent pedestal could be the ultimate limit on the contrast available from ultra-intense laser systems.